scientific reports

Check for updates

OPEN

A weighted gene co-expression network analysis characterises the common defence responses of *Eucalyptus* to diverse biotic challenges

Shae Swanepoel & Sanushka Naidoo✉

Eucalyptus **is a globally important forestry genera cultivated for paper, pulp and biofuel production. These trees are increasingly threatened by a range of emerging pests and pathogens. While previous studies have focused on the transcriptomes of single *Eucalyptus*-pathogen interactions, the core transcriptional networks underlying defence across multiple biotic challenges remain poorly understood. Here we integrated 180 *Eucalyptus*-biotic stress RNA-sequencing libraries to characterise the common defence gene network during interactions with five distinct pathosystems. We constructed a comprehensive weighted gene co-expression network and identified 38 modules of highly co-expressed genes consisting of between 40 and 3,328 genes. The network revealed distinct modules that were induced by pathogen infection, enriched for defence responses including salicylic acid signalling and secondary metabolite biosynthesis and notably nitrate transport and responses, suggesting a potential link between nitrogen metabolism and immunity. Transcription factor enrichment analysis highlighted *WRKY* family genes as key regulators of induced responses, with *WRKY6* emerging as a candidate hub gene in broad-spectrum resistance. Together, this study provides the first integrative transcriptome network of *Eucalyptus* responses to diverse biotic stressors, and offers candidate genes and pathways for future functional validation to enhance disease resistance resource in long-lived trees.**

Keywords Systems genetics, *Eucalyptus* immunity, Comparative transcriptomics, Common defences, Biotic stress

Plants have evolved complex immune systems in response to diverse biotic threats from the environment. Pattern-triggered immunity (PTI) is an initial broad-spectrum response that is initiated by the perception of conserved microbial signatures through pattern recognition receptors (PRR) while effector-triggered immunity (ETI) involves a more robust and sustained response triggered by nucleotide-binding leucine-rich repeat (NLR) proteins recognising pathogen effectors[1]. These pathways were previously considered distinct, but several studies have shown extensive crosstalk and coordination among these responses to initiate robust immunity[2–4]. Furthermore, studies have shown that effectors from pathogens with diverse lifestyles target broad sets of host defence proteins[5], suggesting a centralised plant defence gene architecture. While these mechanisms have been extensively studied in model plants like *Arabidopsis*, their characterisation in long-lived woody species is less understood.

Eucalyptus are a globally important forestry genus that is cultivated for paper, pulp and biofuel. Comprising over 700 species and hybrids, this fast-growing crop exceeds 22.57 million hectares of plantations globally[6,7]. Their sustainability is threatened by various pests and pathogens, with novel threats emerging as a direct result of increased anthropogenic activity, such as increased global trade of eucalypt products[8,9]. Biotic threats of *Eucalyptus* include (i) the myrtle rust pathogen *Austropuccinia psidii*[10], characterised by yellow pustules of urediniospores on emerging leaves and stems[11]; (ii) the necrotrophic stem canker pathogen *Chrysoporthe austroafricana*[12], which causes stem cankers and girdling in susceptible *Eucalyptus* spp.[13]; (iii) the hemi-biotrophic pathogen *Teratosphaeria destructans*[14], responsible for leaf and shoot blight leading to defoliation

Department of Biochemistry, Genetics and Microbiology, Forestry and Agricultural Biotechnology Institute (FABI), University of Pretoria, Pretoria, South Africa. ✉email: sanushka.naidoo@fabi.up.ac.za

and plant death[15]; (iv) the oomycete pathogen *Phytophthora cinnamomi* that causes root and collar rot, leading to tree mortality in cold tolerant *E. nitens*[16]; and (v) the insect pest *Leptocybe invasa* which forms galls on leaves, petioles and stems of young *Eucalyptus*[17].

The molecular interactions between *Eucalyptus* and these biotic threats have been extensively studied. These include transcriptome and proteome analysis of the interactions between *E. urophylla* × *E. tereticornis* and the necrotrophic fungal pathogen, *Calonectria pseudoreteaudii*[18]; *E. grandis* in response to the myrtle rust pathogen *A. psidii*[19,20]; *Eucalyptus* transcriptomes in response to *L. invasa*[21,22]; the transcriptomic responses of *E. camaldulensis* to *Glycaspis brimblecombei*[23]; *E. urophylla* transcriptomes upon infestation with *Ralstonia solanacearum*[24]; and the transcriptome signatures of *Eucalyptus* to the stem canker pathogen *C. austroafricana*[25]. These have provided valuable insights into the tailored defence responses of *Eucalyptus*, but the shared regulatory networks underlying immunity remains poorly understood.

To address this gap, we integrated 180 transcriptomic datasets that span diverse *Eucalyptus* pathosystems (Table 1). Using a weighted gene co-expression network analysis (WGCNA) approach, we aimed to identify core modules and central hubs of defence. We identified induced defence modules associated with salicylic acid, secondary metabolism and nitrate transport and assimilation. Further analysis revealed enrichment of *WRKY* transcription factor genes in the core responses, with *WRKY6* emerging as a putative key regulator. This systems-level approach offers key genes and pathways that serve as candidates for functional validation, which will contribute towards an improved understanding of the molecular mechanisms underlying *Eucalyptus* resilience against pests and pathogens.

Materials and methods

RNA-seq data acquisition

We used a total of 180 previously generated RNA-sequencing libraries (Table 1, Table S1), sourced from the NCBI Short Read Archive and unpublished data generated by our research group. These mRNA-sequencing libraries were generated from different *Eucalyptus* species and hybrids under different biotic and abiotic conditions. This includes *Eucalyptus* responses to *A. psidii*[20], *C. austroafricana*[25,26], *T. destructans*[27] (Motete et al., *in preparation*), *P. cinnamomi*[28] and *L. invasa*[21,22]. All datasets included mock-inoculated and inoculated treatments, with Teshome et al.[26] including water stress in combination with *C. austroafricana* inoculation. Additionally, the datasets included resistant and susceptible host responses (Table 1, Table S1). Throughout this paper, each distinct transcriptomic dataset corresponding to a specific pathogen-host interaction is referred to as a pathosystem.

RNA-seq data quality control and gene expression analysis

The quality of the raw RNA-seq libraries was assessed using FASTQC v0.7.11[29]. Poor quality reads and adapter sequence contamination were trimmed using Trimmomatic v0.36[30] and MultiQC[31] was then used to assess the overall quality of the reads after processing. The *E. grandis* v2.0 reference genome was downloaded from Phytozome v13[32,33] and the quality-filtered reads from each dataset were individually aligned to the reference using Spliced Transcript Alignment to a Reference (STAR) v2.7.10b with default parameters[34] (Fig. 1). StringTie v1.3.4d[35] was used to quantify the read counts as a measure of transcripts per million (TPM) (Fig. 1). The read counts were imported into R v4.3.2[36] using tximport v1.180[37] for further processing. Transcripts with read counts lower than 20 in at least three libraries were filtered to remove low confidence genes, with each pathogen dataset analysed individually. High-quality reads for each pathosystems were analysed individually using DESeq2 v1.40.1[38] (Fig. 1) to identify significantly differentially expressed (DE) genes by comparing inoculated and mock-inoculated datasets. Genes were considered significantly differentially expressed with a Benjamini & Hochberg false discovery rate (FDR) of $p < 0.05$ and an absolute $\log_2$ fold change > 1.0 (Fig. 1).

Transcriptome comparisons

To identify overlapping differentially expressed genes between conditions and gain insights into the commonly differentially regulated genes, the sets of differentially up- and down-regulated genes for each experiment were divided into lists for further comparisons, as described by du Toit et al.[39]. These lists were used to identify

Host species	Interaction	Lifestyle	Tissue type	Libraries	Treatment	Responses	Reference
E. grandis	*A. psidii*	Biotroph	Foliar	48	MI-I	R & S	[20]
E. grandis	*C. austroafricana*	Necrotroph	Stem	12	MI-I	R & S	[25]
E. grandis	*C. austroafricana*	Necrotroph	Stem	38	MI-I; WS-WW	R	[26]
E. grandis	*T. destructans*	Hemi-biotroph	Foliar	24	MI-I	S	[27]
E. grandis	*T. destructans*	Hemi-biotroph	Foliar	16	MI-I	R	Motete et al., *in preparation*
E. grandis × *E. camaldulensis*	*L. invasa*	Insect pest	Foliar	12	MI-I	R & S	[22]
E. grandis × *E. camaldulensis*	*L. invasa*	Insect pest	Foliar	24	MI-I	S	[21]
E. nitens	*P. cinnamomi*	Necrotroph	Stem	6	MI-I	S	[28]

Table 1. A list of *Eucalyptus* transcriptomic datasets used for this study indicating the total number of libraries for each, the treatment applied and the responses of the host. MI – mock-inoculated; I – inoculated; WS – water-stressed; WW – well-watered; R – resistant; S – susceptible.

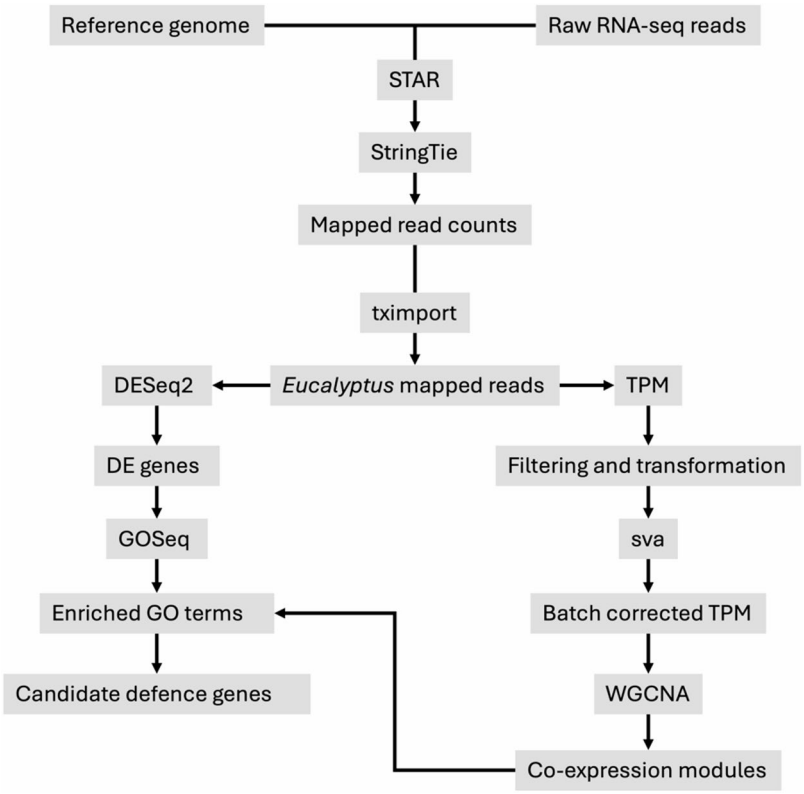

Fig. 1. Flow diagram of the strategy used in this study. DE – differentially expressed. STAR – Spliced Transcript Alignment to a Reference. sva – surrogate variance analysis. TPM – transcripts per million. WGCNA – weighted gene co-expression network analysis.

common and tailored genes between pathosystem interactions (*A. psidii*, *C. austroafricana*, *T. destructans*, *P. cinnamomi* and *L. invasa*) (Fig. 1). Overlapping genes were visualised with VennDiagram v1.7.3[40], and gene ontology (GO) enrichment was performed using GOSeq v1.52.0[41] for biological processes (BP) and molecular functions (MF). Terms were considered significantly over-represented with a Benjamini & Hochberg FDR of $p < 0.1$. Data was visualised with ggplot2 v3.4.4[42] and heatmaps were generated with ComplexHeatmap v2.16.0[43].

Data pre-processing for gene co-expression network analysis

TPM matrices for each experiment were combined into a single expression matrix that consisted of 36,349 genes and 180 samples. Stringent trimming and quality control prior to network generation is recommended to allow the integration of datasets generated across different experiments, where varying conditions and biological systems are analysed[44]. Therefore, genes expressed in less than a third of the samples, low variance genes (i.e. genes with a standard deviation below the first quartile across samples) and genes with annotations related to tRNA, rRNA and ribosomal functions were removed. The filtered matrix was then $\log_2$ transformed. To remove sequencing batch effects that exist between the datasets, sva v3.48.0[45] was used. To remove additional covariates that are caused by factors other than sequencing batch, additional covariates included pathosystem, host response, treatment, abiotic stress, tissue type, and time point. To assess the presence of batch effects before and after correction, principal component analysis (PCA) was performed in R. Filtered, transformed and batch corrected data was then used to generate the co-expression network.

Gene co-expression network analysis

A weighted gene co-expression network analysis (WGCNA) is an unsupervised statistical tool used to identify modules of highly co-expressed genes from which inferences on biological pathways and central hub genes can be made[46]. The pre-processed TPM matrix was used to construct a large-scale gene co-expression network. Similarly to Amrine et al.[44], rather than generating multiple networks for each pathosystem and identifying a consensus network, we generated a single network representative of all datasets. Generating multiple networks would result in reductions of our datasets due to the heterogenous nature of the experimental conditions, with potentially biologically relevant data removed[44].

A signed hybrid adjacency matrix was generated using biweight midcorrelation and a soft-thresholding power of $\beta = 7$ which represented the lowest power required for a scale-free topology of $R^2 = 0.9$ (Fig. S1-S2). The adjacency matrix was used to generate a topological overlap matrix (TOM) to calculate dissimilarity. Modules of co-expressed genes were detected by performing hierarchical clustering based on co-expression dissimilarity

and the dynamic tree cut function was used to identify co-expression modules with a minimum module size of 30, where similar modules were merged using a cut height of 0.25 (Fig. S3).

Module eigengenes (ME) were calculated and used to determine the correlation between modules and traits within the study design, namely: pathosystem (*A. psidii*, *C. austroafricana*, *L. invasa*, *P. cinnamomi* and *T. destructans*); treatment (uninoculated, mock-inoculated, and inoculated); and host response (resistant and susceptible). Abiotic stress, tissue type, and time points were not considered for this study. Finally, gene significance (GS), a measure of correlation between genes and samples, were calculated for each gene in every module. To identify hub genes, a stringent MM threshold ($|MM| > 0.8$) and a more relaxed GS threshold ($|GS| > 0.2$) was used, with these parameters selected to give more weight to the importance of a gene within each module[46].

Module gene enrichment analysis

Genes associated with each module were extracted and used to determine enriched pathways, including GO enrichment, transcription factor (TF) enrichment, TF binding site (TFBS) enrichment and phytohormone gene set enrichment analysis. GO enrichment was performed as described above and results were visualised using GO-Figure v1.0.2 with default parameters[47]. The *E. grandis* TF and phytohormone genes were downloaded from the Plant Transcription Factor Database v5.0 (PlantTFDB) and the Plant Hormone Gene Database (PHGD), respectively[48,49]. Enrichment of genes within each module was determined using a Fisher's exact test with a Benjamini & Hochberg FDR $p < 0.1$ for both TF and phytohormone genes. Finally, to identify over-represented motifs within the promoter regions of the genes of interest, the sequences 1,500 bp upstream of the transcriptional start site (TSS) was extracted as described by Oates et al.[21] using bedtools v2.31.1[50]. These sequences were filtered to ensure the regions did not overlap with neighbouring genes and to remove sequences less than 100 bp in length. The *E. grandis* TF binding motifs were downloaded from the PlantTFDB[48] and used to identify enriched motifs with Analysis of Motif Enrichment v5.5.5 (AME)[51] and a Fisher's exact test with an e-value < 0.0001 of module genes relative to the genome.

Network visualisation and annotations

The co-expression networks were visualised using the igraph package v2.1.2 in R[52]. For the modules of interest, an undirected graph was constructed from the module-specific adjacency matrix generated by WGCNA. To focus on biologically significant nodes, subgraphs were generated with the genes of interest, namely: hub genes; enriched TF; TF genes with enriched binding motifs; and enriched differentially expressed phytohormone genes. Nodes were categories based on functional annotations and their overlap with these gene lists.

Results

Transcriptome comparisons

Differentially expressed genes (DEGs) were identified for each dataset (Table S2), allowing transcriptome comparisons to determine the tailored and shared genes across the different experimental dataset focusing on pathosystem interactions. The greatest number of DE genes were identified in the *T. destructans* susceptible response, with 9,126 up-regulated and 8,943 down-regulated (Fig. 2A), while the *L. invasa* resistant response had the fewest with 952 and 914 up- and down-regulated, respectively (Fig. 2A).

A total of 587 DEGs were shared between the pathosystems (Fig. 2B), representing putative core defence responses. These shared genes were enriched for defence-related responses including phytohormone signalling and reactive oxygen species (ROS) bursts (Fig. 2C, Table S3). Notably, nitrate transport and response to nitrate were terms significantly enriched among these shared genes (Fig. 2C, Table S3). These included *pathogenesis-related (PR)* genes *PR3* and *PR4*, TFs such as *WRKY9* and *WRKY65* and enzyme-associated genes *peroxidase superfamily*, *glycosyl hydrolase* and *laccase* (Table S4).

Nitrate transport has previously been associated with the defence response in *Eucalyptus*[39]. Thus, we further investigated the nitrate transport and assimilation pathway and found 23 DEGs involved in nitrate-related processes (Fig. 3). *Nitrate transporter (NRT)* genes involved in xylem loading, phloem loading, nitrate uptake and vacuole storage were DE upon pathogen challenge. Among these, *NRT1.5 (Eucgr.E01723)*, associated with xylem loading, was strongly induced upon pathogen challenge (Fig. 3). Similarly, *NRT3.1 (Eucgr.B00213)* and *NRT2.5 (Eucgr.H02533)* were among the 587 shared pathosystem interaction DEGs (Table S4), suggesting nitrate transport plays a central role in *Eucalyptus* defences. Finally, the nitrogen assimilation pathway included extensive reprogramming of genes following pathogen infection (Fig. 3), with differential patterns observed in resistant and susceptible hosts, suggesting a potential trade-off between defence and growth (Fig. 3).

Co-expression network analysis and module gene enrichment

While it is valuable to gain an insight into the general expression patterns among the pathosystems, transcriptome comparisons do not explore the relationships among expressed genes. Therefore, to better understand the complex biological network associated with defence upon pathogen challenge, a comprehensive co-expression network was generated.

Generation of a high-quality co-expression network

A major challenge when generating co-expression networks with datasets that have varying conditions and biological systems is the biases that may be introduced due to data heterogeneity[44]. Therefore, we implemented stringent pre-filtering, followed by quality assessments to determine the optimal parameters for network construction. Out of the 34,349 genes, 7,642 were filtered out for low expression, 7,177 for low variance (< 25%) and 707 with annotations related to tRNA, rRNA and ribosomal function. This resulted in a final matrix of 21,118 genes for network construction.

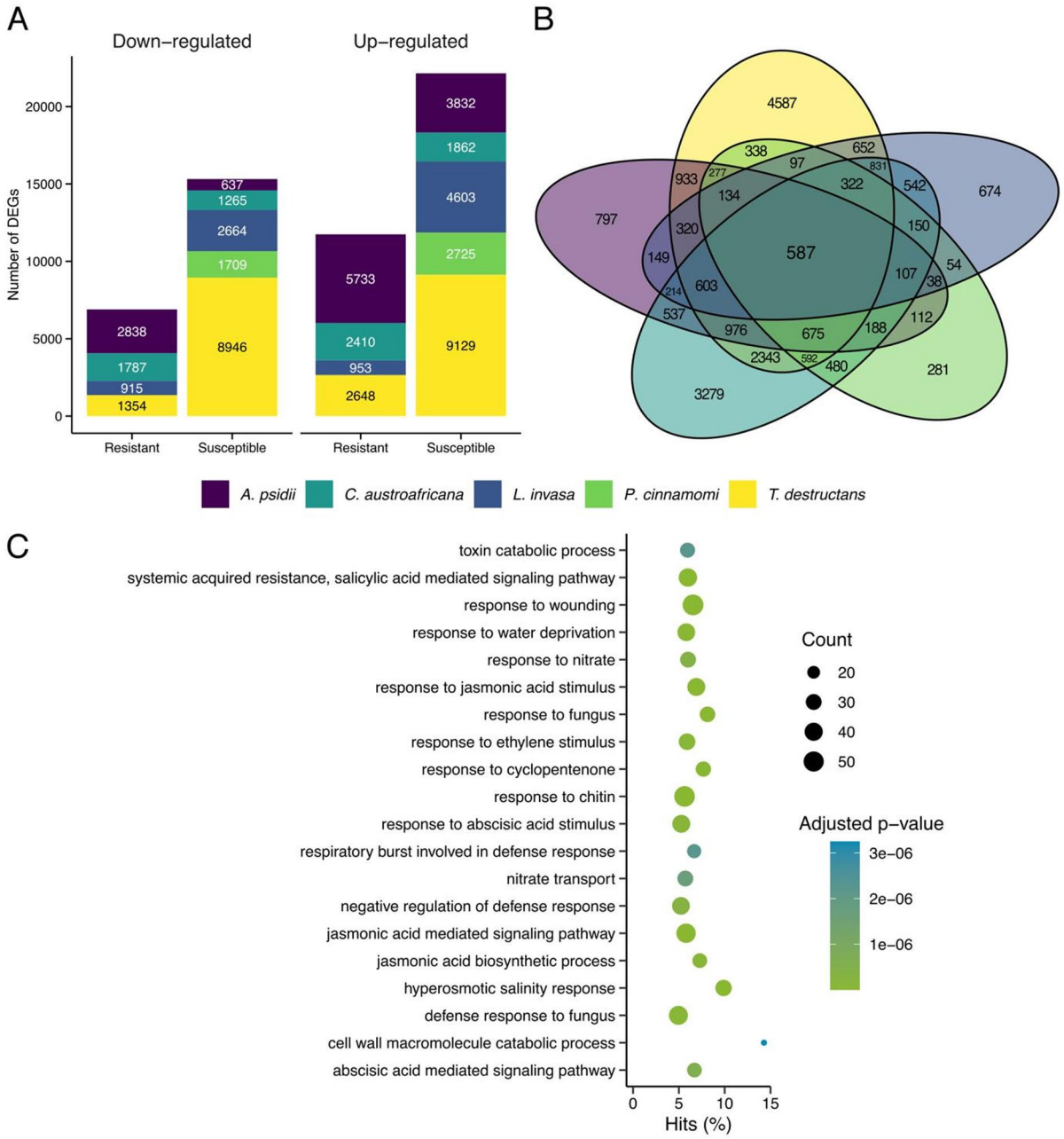

Fig. 2. Transcriptome comparisons for each pathosystem interaction. (**A**) Distribution of the significantly differentially expressed genes in the resistant and susceptible hosts across the interactions. The graph is divided into up- (right) and down-regulated (left) genes. (**B**) Venn diagram showing the overlapping significantly differentially regulated genes between the pathosystems, showing 587 genes shared between the pathosystems. (**C**) The top 20 biological processes gene ontology (GO) enrichment of the 587 overlapping genes between the pathosystems. The count represents the number of genes in each category showing the adjusted *p*-value by colour. Hits represent the percentage of genes within each category, calculated by dividing the cluster genes per category by the total genes per category.

Quality control of the libraries identified five outliers (four *T. destructans* and one *A. psidii*), resulting in 175 libraries for network construction. These were removed from subsequent analyses (Fig. S4). Principal component analysis (PCA) showed that ca. 29% of variation was associated with sequencing batches, where PC2 appeared to separate by pathosystem (Fig. S5A). After batch correction, this separation was reduced (PC2 = 15.7%) (Fig. S5B), though *C. austroafricana* drought-stress samples still clustered distinctly, which may be explained by the combination of biotic and abiotic stress conditions (Fig. S5B). Due to the biological relevance of these samples, they were not removed from the matrix.

The scale independence and mean connectivity over a range of powers was investigated to determine the optimal soft-thresholding power for network construction (Fig. S1)[46]. Given the size of the matrix and

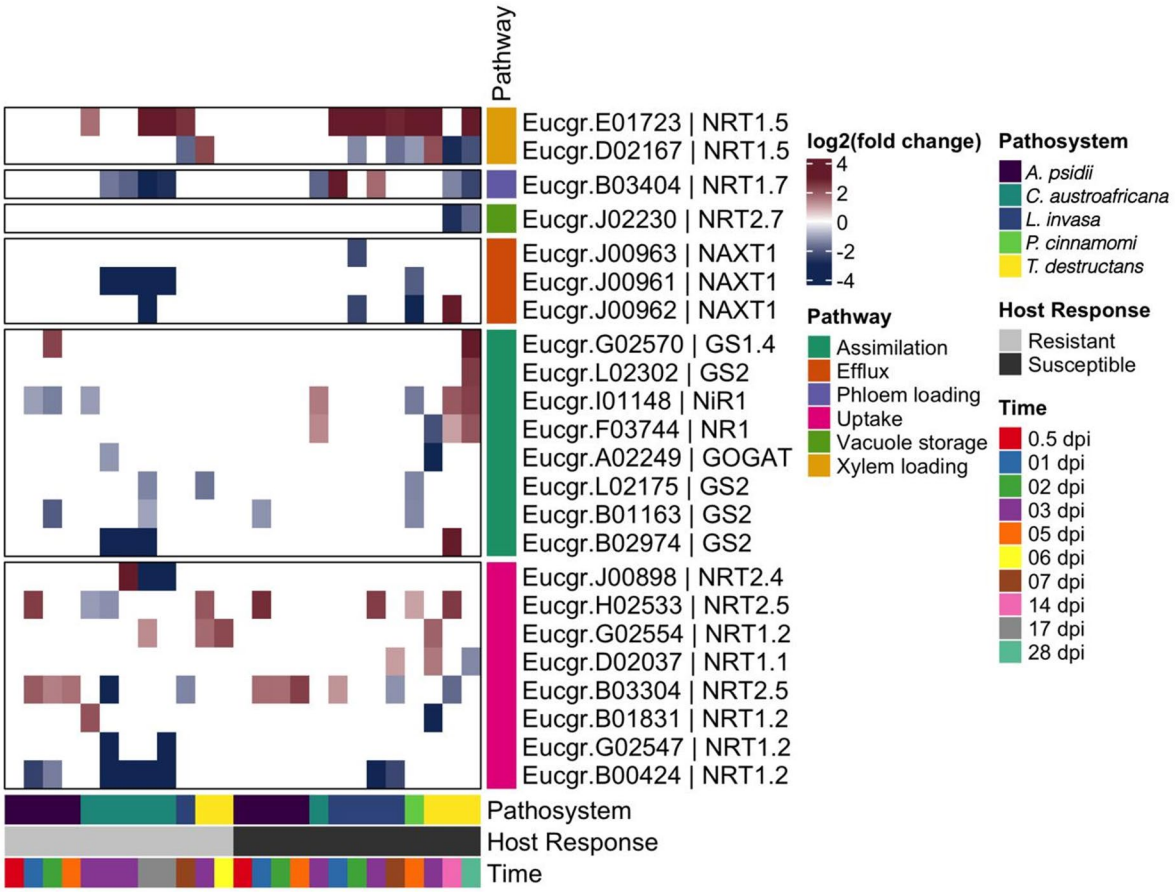

Fig. 3. Heatmap showing the differential expression of nitrate transport and assimilation genes across each pathosystem. Resistant hosts are represented by the grey bar and susceptible hosts are represented by the black bar. Pathways include assimilation, efflux, phloem loading, uptake, vacuole storage and xylem loading. Red and blue represents up- and down-regulated genes, respectively. GOGAT – glutamine-2-oxoglutarate aminotransferase; GS – glutamine synthetase; NAXT – nitrate excretion transporter; NiR – nitrite reductase; NR – nitrate reductase; NRT – nitrate transporter.

heterogeneity of the data, the scale independence and mean connectivity reflect the robustness of the network. Furthermore, the histogram of connectivity showed most genes had low connectivity and few highly connected hub genes (log-log R^2 = 0.84, slope = -2), indicative of a scale-free network (Fig. S2). These evaluations satisfy the assumptions necessary for weighted network construction[46], confirming the data is well-suited to extract biologically meaningful data. The final network identified a total of 38 modules of co-expressed genes, ranging from 40 to 3,328 genes (Fig. S3 and Fig. S6). Many of these modules contained DEGs identified in the transcriptome analysis, underscoring their relevance in defence (Fig. S6, Table S2). Modules significantly correlated with the traits of interest were selected for downstream analyses (Table S5).

Co-expression modules associated with core defences

Two modules, M05 (1,530 genes) and M07 (1,052 genes) showed strong induction upon pathogen challenge (M05 inoculated $r = 0.59$, $p = 1E\text{-}17$; M07 inoculated $r = 0.56$, $p = 1E\text{-}15$; Table S5), consistent with their putative roles as core defence modules. Heatmaps and eigengene expression plots revealed the overall expression was lower in the mock-inoculated and uninoculated compared to the inoculated samples, with expression increasing upon pathogen challenge (Fig. S7-S8).

In module M05, approximately 95% (1,454) genes were significantly differentially regulated, and expression of genes was generally higher in *A. psidii* and *C. austroafricana* (Fig. S7). M05 was enriched for defence pathways (Fig. 4A), including phytohormone processes involving ethylene (ET), salicylic acid (SA), jasmonic acid (JA) and abscisic acid (ABA) (Table S6-S7). Further investigations of the phytohormone-associated genes revealed M05 had a plethora of DE SA-associated genes involved in biosynthesis, signalling and perception of this hormone (Table S8). Notably, nitrate transport and response to nitrate were significantly enriched, corroborating the patterns observed in the transcriptome comparisons (Fig. 4A). This module harboured 20 *WRKY* TF genes, including *WRKY6 (Eucgr.K00786)*, in addition to WRKY/NAC/bHLH binding sites (Table 2 and Table S9). Hub genes included DE *NAD(P)-binding Rossman-fold superfamily protein (Eucgr.K01709)*, a *leucine-rich repeat protein kinase family protein* gene *(Eucgr.B00556)*, an *MLP-like protein 423 (Eucgr.H04007)* and a *pathogenesis-*

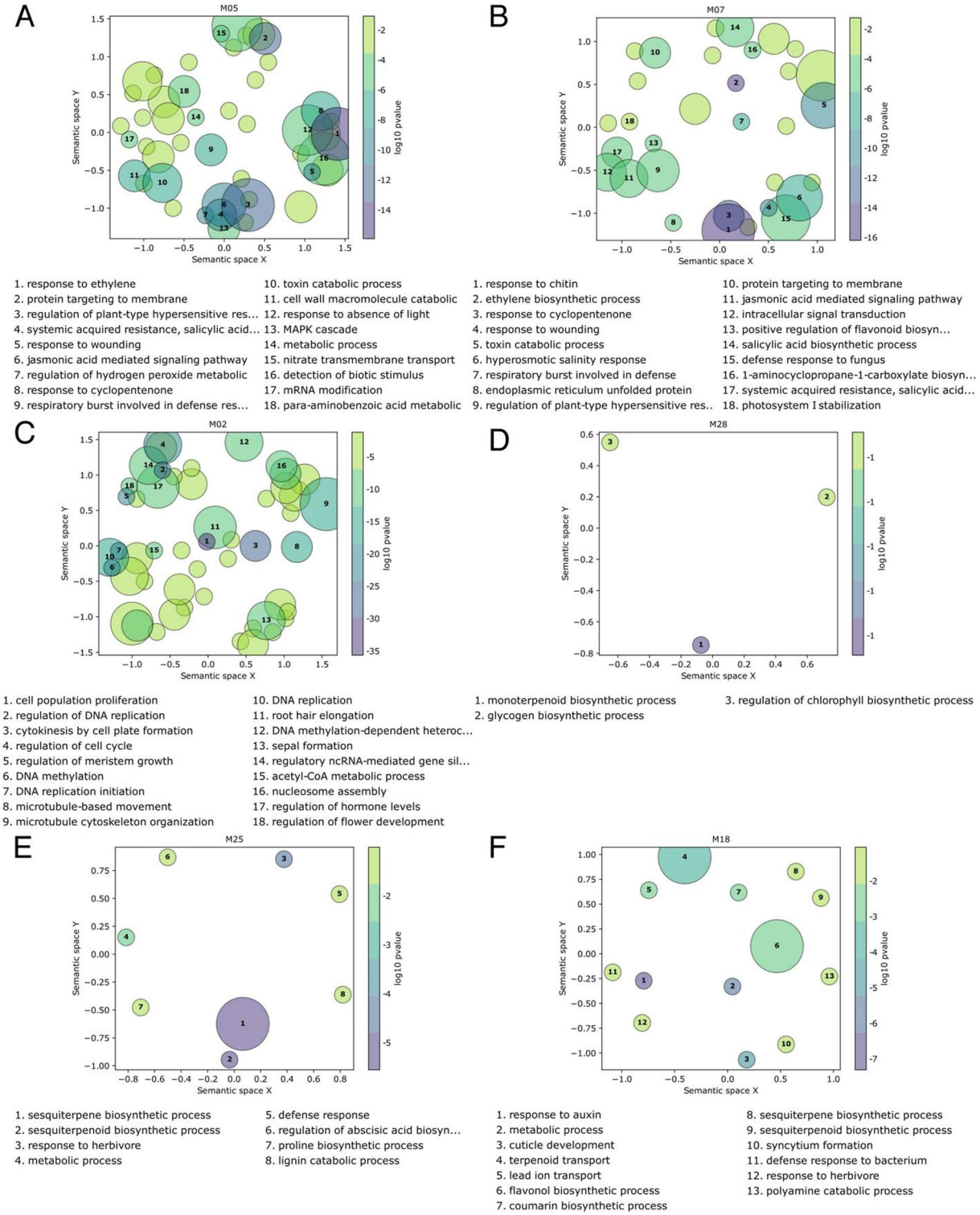

Fig. 4. Semantic similarity scatterplots represented enriched biological processes (BP) gene ontology (GO) terms for the modules of interest. Circles and circle size represent similarity between GO terms and the number of enriched terms, respectively, with colour representing $\log_{10}p$-value. (**A**) M05 ($n = 1{,}530$), (**B**) M07 ($n = 1{,}052$), (**C**) M02 ($n = 2{,}660$), (**D**) M28 ($n = 138$) and (**E**) M25 ($n = 286$) and M18 ($n = 286$).

Module	TF family	Adjusted *p*-value	Gene ID	Gene name
M02	AP2	0.005735122	Eucgr.B02453	RAP2.7, TOE1
			Eucgr.C02333	AIL5, CHO1, EMK
			Eucgr.F00098	ANT, CKC1, DRG
			Eucgr.F02223	ANT, CKC1, DRG
			Eucgr.F04421	-
			Eucgr.G02636	ASML1, WRI1
			Eucgr.H02335	ANT, CKC1, DRG
			Eucgr.J02113	RAP2.7, TOE1
	GRF	0.02131437	Eucgr.A01418	GRF7
			Eucgr.A01534	GRF4
			Eucgr.C00823	GRF5
			Eucgr.F00097	GRF1
	SBP	0.003956584	Eucgr.B00631	-
			Eucgr.B03518	-
			Eucgr.E01600	SPL8
			Eucgr.E03260	SPL5
			Eucgr.K01046	SPL5
			Eucgr.K01828	SPL9
			Eucgr.K02708	-
M05	RAV	0.016148197	Eucgr.B03048	EDF1,TEM1
			Eucgr.D00053	EDF1,TEM1
			Eucgr.L01673	EDF1,TEM1
	WRKY	3.72E-09	Eucgr.B03520	WRKY75
			Eucgr.B04010	WRKY26
			Eucgr.C02659	WRKY40
			Eucgr.C04011	WRKY11
			Eucgr.D01605	WRKY40
			Eucgr.D01811	WRKY27
			Eucgr.E02783	WRKY65
			Eucgr.F03955	WRKY40
			Eucgr.F04317	WRKY40
			Eucgr.G02469	WRKY3
			Eucgr.H03349	WRKY75
			Eucgr.H04061	WRKY23
			Eucgr.I00316	WRKY51
			Eucgr.I00317	WRKY51
			Eucgr.I01633	WRKY75
			Eucgr.I01998	WRKY4
			Eucgr.J01756	WRKY23
			Eucgr.J03117	WRKY40
			Eucgr.K00786	WRKY6
			Eucgr.K02453	WRKY72
M07	C2H2	0.053392461	Eucgr.A01231	-
			Eucgr.A01232	-
			Eucgr.A02369	-
			Eucgr.B02487	-
			Eucgr.B02564	-
			Eucgr.B03372	ZFP5
			Eucgr.C01586	STOP1
			Eucgr.C01587	STOP1
			Eucgr.G02910	-
			Eucgr.J02278	-
	NAC	0.005086687	Eucgr.A02074	NAC046
			Eucgr.D00594	NAC073, SND2
			Eucgr.D00595	NAC073, SND2
			Eucgr.D02182	NAC071

Continued

Module	TF family	Adjusted *p*-value	Gene ID	Gene name
			Eucgr.F01539	NAC079, NAC4, NAC080
			Eucgr.F04341	NAC002, ATAF1
			Eucgr.G01758	NTL9
			Eucgr.H03387	NAC083, VNI2
			Eucgr.I00057	NAC102
			Eucgr.I00095	NAC002, ATAF1
			Eucgr.I00098	NAC102
			Eucgr.I00101	NAC002, ATAF1
			Eucgr.I02695	NAC104, XND1
			Eucgr.J00520	NAC090
			Eucgr.K01472	NAC087
	ERF	0.000293842	Eucgr.B03559	Rap2.6 L
			Eucgr.C02719	-
			Eucgr.C03175	-
			Eucgr.E00834	CRF2, TMO3
			Eucgr.E02651	ERF2
			Eucgr.E03168	ERF1
			Eucgr.F02317	RAP2.1
			Eucgr.F04203	-
			Eucgr.G00393	EREBP, ERF13
			Eucgr.G01970	Rap2.6 L
			Eucgr.H01085	HRE2
			Eucgr.H03965	EBP, ERF72, RAP2.3
			Eucgr.H04892	Rap2.6 L
			Eucgr.I00291	-
			Eucgr.K02193	-
	WRKY	0.000156337	Eucgr.A01990	WRKY28
			Eucgr.A02718	WRKY27
			Eucgr.C00077	WRKY11
			Eucgr.D00336	WRKY28
			Eucgr.E04011	WRKY6
			Eucgr.F00740	WRKY6
			Eucgr.H00996	WRKY23
			Eucgr.H04135	WRKY42
			Eucgr.I00882	WRKY11
			Eucgr.I01927	WRKY72
			Eucgr.K00331	WRKY41
			Eucgr.K01219	WRKY28

Table 2. Significantly enriched transcription factors in the modules of interest.

related family protein (Eucgr.F02732) (Table S10-S11). Finally, a sub-network identified three highly clustered nodes *(Eucgr.K00786*, *Eucgr.H03349* and *Eucgr.E0278)*, with these among enriched TF, TFBS and SA-associated enriched genes (Fig. 5A), suggesting these are strong regulators within M05.

M07 (91.1% DEGs) exhibited similar patterns to M05, with expression generally higher in *A. psidii* and *C. austroafricana* (Fig. S8). M07 was enriched for SA, JA, brassinosteroid (BR) signalling, phenylpropanoid and flavonoid biosynthesis (Fig. 4B). This module also contained 29 DE SA-associated genes and numerous *WRKY*, *NAC*, *ERF* and *C2H2* TF genes, with *WRKY6* (*Eucgr.E04011*) appearing as an enriched TF, a potential hub and DE in transcriptome comparisons Table 2, Table S10-S11). The sub-network was sparser than for M05 but revealed a distinct overlap between hub genes and enriched SA-associated genes (Fig. 5B).

Module associated with constitutive expression

In contrast to M05 and M07, M02 (2,660 genes) had higher expression in mock-inoculated samples and expression was reduced upon infection, indicative of constitutive growth and development functions down-regulated during defence (mock-inoculated $r = 0.35$, $p = 3E\text{-}06$; Table S5 and Fig. S9). In general, heatmap and eigengene expression plots showed expression of these genes was lower in resistant compared to susceptible hosts (Fig. S9). Genes for growth and development are constitutively expressed in mock-inoculated samples and greater expression in susceptible hosts suggests these plants are unable to effectively regulate between growth and defence trade-offs. Enrichment included pathways involved in growth and development, including BR

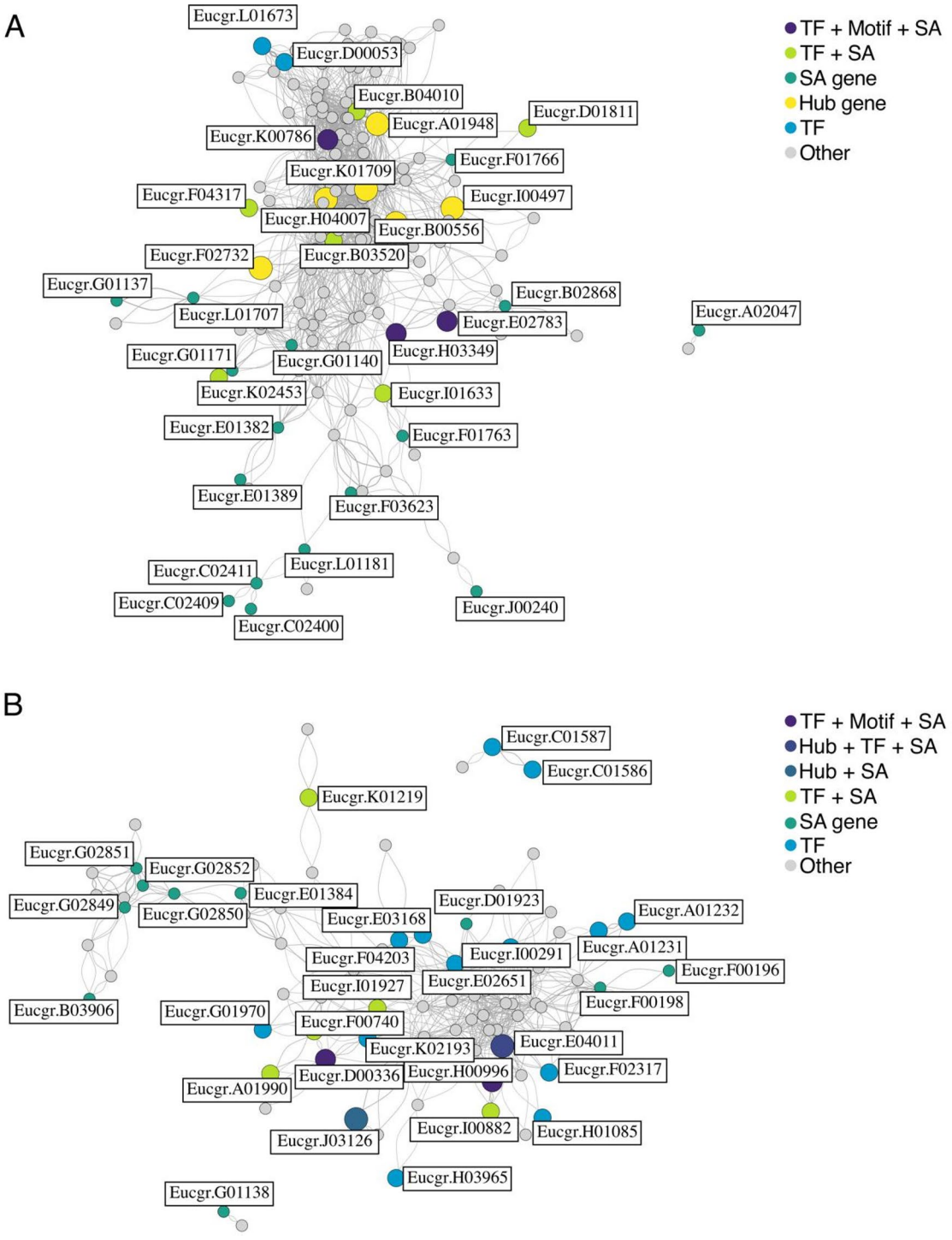

Fig. 5. Network analysis of co-expression modules associated with core defences in *Eucalyptus*. Each subnetwork displays only the first-degree neighbours of genes of interest: hub genes, enriched transcription factors (TF), genes with enriched TF binding motifs, and enriched salicylic acid (SA)-associated genes. Nodes are coloured according to functional annotation categories. (**A**) Module M05 shows a dense subnetwork including multiple overlapping regulatory roles among the genes of interest. (**B**) Module M07 reveals TFs and SA-associated genes.

biosynthesis, auxin signalling, plant growth and plant-type cell wall biogenesis (Fig. 4C, Table S6-S7). Enriched TFs included *GRF*, *AP2* and *SBP* (Table 2). M02 had a significant number of hub genes (Table S10) including a *leucine-rich repeat protein kinase family protein* gene (*Eucgr.B00412*) DE in the transcriptome comparison analysis (Table S11).

Modules associated with pathosystem-specific responses

Module M28 (138 genes) was significantly correlated with *A. psidii*, *T. destructans* and *C. austroafricana* (*A. psidii* $r = 0.41$, $p = 3E\text{-}08$; *T. destructans*, $r = 0.56$, $p = 5E\text{-}16$ and *C. austroafricana*, $r = -0.78$, $p = 2E\text{-}36$; Table S5). The expression of these genes was higher in *A. psidii* and *T. destructans* and lower in *C. austroafricana* (Fig. S10). This module was enriched for genes involved in monoterpenoids biosynthesis and terpenoid synthase activity (Fig. 4D, Table S6). Fifteen hub genes were identified, including a *GATA type zinc finger transcription factor family protein* gene (*Eucgr.C03895*) (Table S10).

Module M38 (40 genes), the smallest module, showed interesting expression patterns for *T. destructans* ($r = 0.73$, $p = 6E\text{-}30$; Table S5), with eigengene expression greater in all *T. destructans* samples and greater in resistant samples (Fig. S10-S11). Additionally, eigengene expression was greater in resistant samples. Genes within this module included an *NB-ARC domain containing disease resistance protein* gene *(Eucgr.E01278)*, a *cysteine-rich receptor-like kinase protein* gene *(Eucgr.E04192)*, and a *terpene synthase-like 1,8-cineole* gene *(Eucgr.L02212)*. These genes were differentially regulated in responses to *T. destructans* in the transcriptome comparison analysis (Table S2). Although small and lacking enrichments, its expression patterns strongly suggest a role in specific resistance to *T. destructans.*

Modules associated with resistance and susceptibility

M25 (185 genes) was most correlated with susceptibility ($r = 0.59$, $p = 9E\text{-}18$; Table S5). Eigengene expression was greater in susceptible *L. invasa* mock-inoculated and inoculated samples ($r = 0.53$, $p = 4E\text{-}14$; Fig. S12, Table S5). This module was enriched for terms typically associated with herbivore stress, including response to herbivore, sesquiterpene biosynthesis, monoterpene synthesis, and the lignin catabolic process (Fig. 4E, Table S6). Of the total hub genes identified in all the modules of interest, 77 were found in M25 and 54 were significantly DE (Table S10-S11). Five of these were annotated as *terpene synthase* genes, namely *Eucgr.E03570*, *Eucgr.C02489*, *Eucgr.F03398*, *Eucgr.E02670*, *and Eucgr.L03538* (Table S10).

M18 (286 genes) was also linked to susceptible samples ($r = 0.42$, $p = 7.00E\text{-}09$) (Table S5), with associations with foliar pathogens *A. psidii* and *L. invasa* (Fig. S13). Enriched terms included specialised metabolites including terpenoids, flavanols, and sesquiterpenes as well as phytohormones including abscisic acid and auxins (Fig. 4F, Table S6-S7). This highlights distinct transcriptional profiles in susceptible hosts.

Discussion

This study integrated a range of transcriptomic datasets to generate a robust co-expression network across five *Eucalyptus* pathosystems to dissect the core and tailored defence responses. We found genes involved in nitrate transport, SA signalling and WRKY TFs as key components of the induced defence network, along with modules with tailored responses to specific pathosystems and trade-offs between growth and immunity.

A central finding is the recurring involvement of nitrate transport and assimilation, SA signalling and WRKY TFs genes across multiple pathosystems, indicating these as a core component in *Eucalyptus* immunity. The identification of *NRT2.5* and *NRT3.1* among the 587 shared DEGs across all pathosystems suggests the coupling of nutrient allocation with defence (Fig. 3, Table S2) especially given that NRT3.1 forms a tetrameric complex with NRT2.5 to facilitate the high-affinity uptake of nitrates[53]. Numerous studies have associated NRT2 family members with biotic stress. du Toit et al.[39] showed that inactivation of *NRT2.5* improves *Arabidopsis thaliana* resistance to *Psuedomonas syringae* pv. *tomato* DC3000 (*Pst*). A *nrt2.1* mutant *A. thaliana* had reduced sensitivity to coronatine and rapid priming of SA, leading to improved tolerance to *Pst* infection[54]. The exact role these genes play in the defence response of *Eucalyptus* remains unclear, representing an important avenue for functional studies.

Investigating additional nitrate uptake and assimilation genes revealed extensive transcriptomic changes upon pathogen perturbation (Fig. 3). This included eight nitrogen assimilation genes, namely *nitrate reductases* (*NR*), *nitrite reductases* (*NiR*) and amino acid assimilation genes in the *glutamine synthetase/glutamine-2-oxoglutarate aminotransferase* (*GS/GOGAT*) cycle (Fig. 3)[55]. Several studies have investigated the impact that this assimilation cycle has on plant immunity. In rice, *gogat* mutants showed resistance to multiple strains of *Xanthomonas oryzae* pv. *oryzae*[56]. In *Solanum lycopersicum*, silencing of *NR*, *NiR* and *GOGAT* resulted in increased resistance against two bacterial pathogens, *P. syringae* and *Ralstonia solanacearum*[57]. Interestingly, this silencing resulted in an increase in SA levels, as well as an up-regulation of SA biosynthesis and signalling genes *PAL1*, *PR2* and *PR4* in inoculated plants[57], with the authors postulating that SA-mediated defences act downstream of nitrogen metabolism.

Our co-expression network identified modules (M05 and M07) induced upon pathogen challenge, enriched for SA, JA, ET and ABA pathways (Table S7). Notably, these modules contained over 80 significantly DE and enriched SA-related genes, compared to only five associated with JA (Table S8). *WRKY* hub genes and *PR-1* signalling were particularly enriched (Table S8), suggesting SA signalling acts a key hub across different *Eucalyptus* interactions. Notably, *WRKY6 (Eucgr.E04011)* was consistently up-regulated across all pathosystems and has been shown to be involved in enhancing broad-spectrum resistance in plant species via SA-signalling[58,59]. While SA signalling has been traditionally associated with defence against (hemi)-biotrophs[60], this study complements others[61–64] to suggest that SA contributes to resistance against pathogens with diverse lifestyles, particularly in woody perennial species. Indeed, marker genes associated with SA signalling and systemic acquired resistance (SAR) in *Eucalyptus* were up-regulated in response to the necrotrophic fungal pathogen *C. austroafricana*[25,65,66]. Additionally, a plethora of *PR* genes associated with SA signalling were also up-regulated in *Eucalyptus* infected with the root rot pathogen, *P. cinnamomi*[28]. Taken together, these findings suggest that SA and the establishment of SAR may form a key part of the core defence network in *Eucalyptus*[67], irrespective of pathogen lifestyle.

Within modules M05 and M07, we identified several key DE hub genes (Table S10-S11). MLP423 has been shown to inhibit the expression of phytohormone-related genes[68] and this gene was up-regulated in

Eucalyptus challenged by *C. pseudoreteaudii*[18]. Members of the NAD(P)-binding Rossman-fold superfamily proteins, classed as metabolic enzymes, enhances resistance to (hemi)-biotrophic pathogens by modulating phytohormone gene expression, such as inducing *PR1* and reducing *LOX1* expression[69,70]. In *Arabidopsis*, a leucine-rich repeat receptor-like kinase orthologous to *NILR1* recognises nematode-derived molecules to initiate broad-spectrum systemic immunity[71,72] was identified as hub gene in a multi-pathogen co-expression network in *Arabidopsis*[44]. A pathogenesis-related protein family (PRP1), involved in nitrogen fixation in *Lotus japonicus*, is associated with MAPK cascades and induction of defence-related genes[73], with putative involvement in water-stressed *Eucalyptus*[74]. Finally, HCT, involved in the phenylpropanoid pathway, has been shown to synthesise precursors that lead to the production of lignin in the secondary cell wall structure[75,76]. Moreover, *Eucalyptus* challenged by *C. pseudoreteaudii* had clear transcriptomics alterations in the phenylpropanoid pathway, with this *HCT* contributing to these findings[18], showing its potential role in cell wall strengthening under biotic stress. Together, these hub genes integrate hormone signalling, receptor perception, metabolic reprogramming and structural defences. This highlights them as promising targets for future functional studies to better understand the *Eucalyptus* immune network.

Beyond these core induced responses, our network revealed distinct transcriptional signatures associated with the constitutive expression of growth-associated pathways including auxin signalling (Fig. 4C). This provides molecular support for the growth-defence trade-off hypothesis[77]. Auxin plays an important role in growth and development, yet studies have shown that increased levels lead to plant susceptibility to biotic stress. For example, elevated auxin levels in *A. thaliana* reduced expression of SA-dependent defence genes, resulting in increased bacterial growth of *Pto*[78]. Conversely, constitutive activation of *PR* genes in *A. thaliana* is associated with reduced vegetative growth[79,80]. Together, these studies show the cost of sustained defence and highlight the growth-defence balance.

Similar growth-resistance trade-offs have been reported in trees. For example, *Pinus pinaster* families selected for improved growth were significantly more susceptible to *Hylobius abietis* and *Matsucoccus feytaudi* than unimproved material[81,82]. These observations highlight the importance of considering productivity traits alongside general defence capacity to balance survivability and economic return[83]. While our dataset does not include direct growth phenotypes, the constitutive activation of auxin-related modules suggests a potential allocation trade-off between growth and defence. This warrants targeted investigation in future work integrating both transcriptomic and growth trait data.

Conclusion

The defence responses of *Eucalyptus* are complex and integrated, as highlighted by the co-expression network generated in this study. Here, we have identified both conserved and diverse transcriptional responses to pests and pathogens under different conditions. Although we did not identify strong correlations with phenotypes and gene expression, it is important to consider the heterogenous nature of the data, including the *Eucalyptus* species, invading organisms and spatial-temporal differences. Thus, the correlations identified suggest strong signals of associations and warrant further investigation. Future research should build upon these findings by incorporating *Eucalyptus* pangenome references to capture species-specific transcriptional differences more accurately to refine our understanding of conserved and lineage-specific defence mechanisms.

We have reiterated the importance genes involved with the nitrate transport and assimilation cycle in the defences of *Eucalyptus*. Additionally, SA signalling was significantly enriched in the core defence modules, and previous studies have shown a potential interplay between SA pathways and nitrate metabolism. Notably, *WRKY6*, associated with SA-signalling, was identified as a candidate hub gene, enriched transcription factor and regulator of genes in core defence modules. While the link between nitrate transport and assimilation and SA defences remains tenuous, studies in model organisms point to a potential mechanism that warrants exploration in *Eucalyptus*. However, practical constraints such as the lack of routine transformation protocols for functional validation in *Eucalyptus* limits immediate testing of this hypothesis. Nonetheless, this study provides compelling evidence for the intersection of these pathways at the transcriptional level.

In conclusion, this study presents a robust pipeline for co-expression network analysis in *Eucalyptus* that can be expanded as more transcriptomic data becomes available. Ultimately, our findings contribute to our understanding of the complexities of the defences in *Eucalyptus* and provides valuable targets and hypotheses for future research aimed at improving resilience in this globally important forest tree.

Data availability

Part of the RNA-sequencing datasets used on this study was sourced from unpublished work currently in preparation and is not publicly available at this time. Requests for access to the unpublished data should be directed to the corresponding author. All other datasets were obtained from publicly available sources. No new raw sequencing data were generated.

Received: 11 July 2025; Accepted: 11 December 2025
Published online: 04 February 2026

References

1. Jones, J. D. G. & Dangl, J. L. The plant immune system. *Nature* **444**, 323–329. https://doi.org/10.1038/nature05286 (2006).
2. Dodds, P. N. & Rathjen, J. P. Plant immunity: towards an integrated view of plant-pathogen interactions. *Nat. Rev. Genet.* **11**, 539–548. https://doi.org/10.1038/nrg2812 (2010).
3. Chang, M., Chen, H., Liu, F., Fu, Z. Q. PTI & ETI: convergent pathways with diverse elicitors. *Trends Plant. Sci.* **27**, 113–115. https://doi.org/10.1016/j.tplants.2021.11.013 (2022).

4. Delplace, F., Huard-Chauveau, C., Berthome, R. & Roby, D. Network organization of the plant immune system: from pathogen perception to robust defense induction. *Plant. J.* **109**, 447–470. https://doi.org/10.1111/tpj.15462 (2022).
5. Mukhtar, M. S. et al. Independently evolved virulence effectors converge onto hubs in a plant immune system network. *Science* **333**, 596–601. https://doi.org/10.1126/science.1203659 (2011).
6. Grattapaglia, D. et al. Progress in myrtaceae genetics and genomics: *Eucalyptus* as the pivotal genus. *Tree Genet. Genomes*. **8**, 463–508. https://doi.org/10.1007/s11295-012-0491-x (2012).
7. Seng Hua, L. et al. Engineering wood products from *Eucalyptus* spp. *Adv. Mater. Sci. Eng.* 8000780 (2022). (2022). https://doi.org/10.1155/2022/8000780
8. Wingfield, M. J. et al. Eucalypt pests and diseases: growing threats to plantation productivity. *South. J. Sci.* **70**, 139–144. https://doi.org/10.2989/SOUTH.FOR.2008.70.2.9.537 (2008).
9. Hurley, B. P. et al. Increasing numbers and intercontinental spread of invasive insects on eucalypts. *Biol. Invasions*. **18**, 921–933. https://doi.org/10.1007/s10530-016-1081-x (2016).
10. Beenken, L. A new genus name for the Myrtle rust *Puccinia psidii* placed within the redefined family Sphaerophragmiaceae (Pucciniales). *Phytotaxa* **297**, 53–61. https://doi.org/10.11646/phytotaxa.297.1.5 (2017). Austropuccinia.
11. Coutinho, T. A., Wingfield, M. J., Alfenas, A. C. & Crous, P. W. *Eucalyptus* rust: a disease with the potential for serious international implications. *Plant. Dis.* **82**, 819–825. https://doi.org/10.1094/PDIS.1998.82.7.819 (1998).
12. Gryzenhout, M. et al. *Chrysoporthe*, a new genus to accommodate *Cryphonectria Cubensis*. *Stud. Mycol.* **50**, 119–141 (2004).
13. Conradie, E., Swart, W. J. & Wingfield, M. J. *Cryphonectria* canker of *Eucalyptus*, an important disease in plantation forestry in South Africa. *S Afr. J.* **152**, 43–49. https://doi.org/10.1080/00382167.1990.9629018 (1990).
14. Andjic, V. et al. Multiple gene genealogies reveal important relationships between species of *Phaeophleospora* infecting *Eucalyptus* leaves. *FEMS Microbiol Lett*. **268**, 22–33. https://doi.org/10.1111/j.1574-6968.2007.00637.x (2007).
15. Wingfield, M. J., Crous, P. W. & Boden, D. *Kirramyces destructans* sp. nov., a serious leaf pathogen of *Eucalyptus* in Indonesia. *S Afr. J. Bot.* **62**, 325–327 (1996).
16. Wingfield, M. J. & Knox-Davies, P. Observations on diseases in pine and Eucalyptus plantations in South Africa. *Phytophylactica* **12**, 57–63 (1980).
17. Mendel, Z., Protasov, A., Fisher, N. & La Salle, J. Taxonomy and biology of *Leptocybe Invasa* gen. & sp. n. (Hymenoptera: Eulophidae), an invasive gall inducer on *Eucalyptus*. *Aust J. Entomol.* **43**, 101–113. https://doi.org/10.1111/j.1440-6055.2003.00393.x (2004).
18. Chen, Q. et al. Transcriptome and proteome analysis of *Eucalyptus* infected with *Calonectria pseudoreteaudii*. *J. Proteom.* **115**, 117–131. https://doi.org/10.1016/j.jprot.2014.12.008 (2015).
19. Santos, S. A. et al. Transcriptome analysis of *Eucalyptus grandis* genotypes reveals constitutive overexpression of genes related to rust (*Austropuccinia psidii*) resistance. *Plant. Mol. Biol.* **104**, 339–357. https://doi.org/10.1007/s11103-020-01030-x (2020).
20. Swanepoel, S. et al. Transcriptome analysis of *Eucalyptus grandis* implicates brassinosteroid signaling in defense against Myrtle rust (*Austropuccinia psidii*). *Front. Glob Change*. **4**, 778611. https://doi.org/10.3389/ffgc.2021.778611 (2021).
21. Oates, C. N. et al. Insect egg-induced physiological changes and transcriptional reprogramming leading to gall formation. *Plant. Cell. Environ.* **44**, 535–547. https://doi.org/10.1111/pce.13930 (2021).
22. Oates, C. N. et al. The transcriptome and terpene profile of *Eucalyptus grandis* reveals mechanisms of defense against the insect pest, *Leptocybe invasa*. *Plant. Cell. Physiol.* **56**, 1418–1428. https://doi.org/10.1093/pcp/pcv064 (2015).
23. Patton, M. K. F. et al. Transcriptome and defence response in *Eucalyptus camaldulensis* leaves to feeding by *Glycaspis brimblecombei* Moore (Hemiptera: Aphalaridae): a stealthy psyllid does not go unnoticed. *Aust Entomol.* **57**, 247–254. https://doi.org/10.1111/aen.12319 (2017).
24. Xiaohui, Y. et al. Transcriptome and metabolome profiling in different stages of infestation of *Eucalyptus urophylla* clones by *Ralstonia solanacearum*. *Mol. Genet. Genomics*. **297**, 1081–1100. https://doi.org/10.1007/s00438-022-01903-4 (2022).
25. Mangwanda, R., Myburg, A. A. & Naidoo, S. Transcriptome and hormone profiling reveals *Eucalyptus grandis* defence responses against *Chrysoporthe austroafricana*. *BMC Genom.* **16**, 319. https://doi.org/10.1186/s12864-015-1529-x (2015).
26. Teshome, D. T., Zharare, G. E., Ployet, R. & Naidoo, S. Molecular mechanisms underlying tree host-pathogen interactions under drought stress and subsequent rewatering in *Eucalyptus grandis*. *Plant. Stress*. **14**, 100697. https://doi.org/10.1016/j.stress.2024.100697 (2024).
27. Solís, M., Hammerbacher, A., Wingfield, M. J. & Naidoo, S. Transcriptional responses of *Eucalyptus* to infection by an aggressive leaf blight pathogen reveal the role of host secondary metabolites during pathogen germination. *Plant. Mol. Biol.* **115**, 104. https://doi.org/10.1007/s11103-025-01625-2 (2025).
28. Meyer, F. E. et al. Dual RNA-sequencing of *Eucalyptus nitens* during *Phytophthora cinnamomi* challenge reveals pathogen and host factors influencing compatibility. *Front. Plant. Sci.* **7**, 191. https://doi.org/10.3389/fpls.2016.00191 (2016).
29. Andrews, S. FastQC: a quality control tool for high throughput sequence data. Babraham Bioinformatics, Cambridge, UK (2010). Available at: https://www.bioinformatics.babraham.ac.uk/projects/fastqc/
30. Bolger, A. M., Lohse, M., Usadel, B. Trimmomatic: a flexible trimmer for illumina sequence data. *Bioinformatics* **30**, 2114–2120. https://doi.org/10.1093/bioinformatics/btu170 (2014).
31. Ewels, P., Magnusson, M., Lundin, S., Käller, M. MultiQC: summarize analysis results for multiple tools and samples in a single report. *Bioinformatics* **32**, 3047–3048. https://doi.org/10.1093/bioinformatics/btw354 (2016).
32. Goodstein, D. M. et al. Phytozome: a comparative platform for green plant genomics. *Nucleic Acids Res.* **40**, D1178–D1186. https://doi.org/10.1093/nar/gkr944 (2012).
33. Myburg, A. A. et al. The genome of *Eucalyptus grandis*. *Nature* **510**, 356–362. https://doi.org/10.1038/nature13308 (2014).
34. Dobin, A. et al. STAR: ultrafast universal RNA-seq aligner. *Bioinformatics* **29**, 15–21. https://doi.org/10.1093/bioinformatics/bts635 (2013).
35. Pertea, M. et al. StringTie enables improved reconstruction of a transcriptome from RNA-seq reads. *Nat. Biotechnol.* **33**, 290–295. https://doi.org/10.1038/nbt.3122 (2015).
36. R Core Team. R: A language and environment for statistical computing. R Foundation for Statistical Computing, Vienna, Austria. (2023). Available at: https://www.R-project.org/
37. Soneson, C., Love, M. I. & Robinson, M. D. Differential analyses for RNA-seq: transcript-level estimates improve gene-level inferences. *F1000Research* **4**, 1521. https://doi.org/10.12688/f1000research.7563.2 (2015).
38. Love, M. I., Huber, W. & Anders, S. Moderated estimation of fold change and dispersion for RNA-seq data with DESeq2. *Genome Biol.* **15**, 550. https://doi.org/10.1186/s13059-014-0550-8 (2014).
39. du Toit, Y. et al. eCALIBRATOR: a comparative tool to identify key genes and pathways for *Eucalyptus* defense against biotic stressors. *Front. Microbiol.* **11**, 216. https://doi.org/10.3389/fmicb.2020.00216 (2021).
40. Chen, H., Boutros, P. C. VennDiagram: a package for the generation of highly-customizable Venn and Euler diagrams in R. *BMC Bioinform.* **12**, 35. https://doi.org/10.1186/1471-2105-12-35 (2011).
41. Young, M. D., Wakefield, M. J., Smyth, G. K. & Oshlack, A. Gene ontology analysis for RNA-seq: accounting for selection bias. *Genome Biol.* **11**, R14. https://doi.org/10.1186/gb-2010-11-2-r14 (2010).
42. Wickham, H. *ggplot2: Elegant Graphics for Data Analysis* (Springer, 2016).
43. Gu, Z. Complex heatmaps reveal patterns and correlations in multidimensional genomic data. *Bioinformatics* **32**, 2847–2849. https://doi.org/10.1093/bioinformatics/btw313 (2016).
44. Amrine, K. C., Blanco-Ulate, B. & Cantu, D. Discovery of core biotic stress responsive genes in *Arabidopsis* by weighted gene co-expression network analysis. *PLoS One*. **10**, e0118731. https://doi.org/10.1371/journal.pone.0118731 (2015).

45. Leek, J. T. et al. The sva package for removing batch effects and other unwanted variation in high-throughput experiments. *Bioinformatics* **28**, 882–883. https://doi.org/10.1093/bioinformatics/bts034 (2012).
46. Langfelder, P. & Horvath, S. WGCNA: an R package for weighted correlation network analysis. *BMC Bioinform.* **9**, 559. https://doi.org/10.1186/1471-2105-9-559 (2008).
47. Reijnders, M. & Waterhouse, R. M. Summary visualizations of gene ontology terms with GO-Figure! *Front. Bioinform.* **1**, 638255. https://doi.org/10.3389/fbinf.2021.638255 (2021).
48. Jin, J. et al. PlantTFDB 4.0: toward a central hub for transcription factors and regulatory interactions in plants. *Nucleic Acids Res.* **45**, D1040–D1045. https://doi.org/10.1093/nar/gkw982 (2017).
49. Feng, S. et al. PHGD: an integrative and user-friendly database for plant hormone-related genes. *iMeta* 3, e164 (2024). https://doi.org/10.1002/imt2.164
50. Quinlan, A. R., Hall, I. M. BEDTools: a flexible suite of utilities for comparing genomic features. *Bioinformatics* **26**, 841–842. https://doi.org/10.1093/bioinformatics/btq033 (2010).
51. McLeay, R. C. & Bailey, T. L. Motif enrichment analysis: a unified framework and an evaluation on chip data. *BMC Bioinform.* **11**, 165. https://doi.org/10.1186/1471-2105-11-165 (2010).
52. Csárdi, G. et al. igraph: network analysis and visualization in R (version 2.1.4). *Zenodo* https://doi.org/10.5281/zenodo.7682609 (2025).
53. Kotur, Z. & Glass, A. D. A 150 kDa plasma membrane complex of AtNRT2.5 and AtNAR2.1 is the major contributor to constitutive high-affinity nitrate influx in *Arabidopsis thaliana*. *Plant. Cell. Environ.* **38**, 1490–1502. https://doi.org/10.1111/pce.12496 (2015).
54. Camañes, G. et al. A deletion in *NRT2.1* attenuates *Pseudomonas syringae*-induced hormonal perturbation, resulting in primed plant defenses. *Plant. Physiol.* **158**, 1054–1066. https://doi.org/10.1104/pp.111.184424 (2012).
55. Wang, M., Shen, Q., Xu, G. & Guo, S. New insight into the strategy for nitrogen metabolism in plant cells. *Int. Rev. Cell. Mol. Biol.* **310**, 1–37. https://doi.org/10.1016/b978-0-12-800180-6.00001-3 (2014).
56. Chen, H. et al. The Fd-GOGAT1 mutant gene *lc7* confers resistance to *Xanthomonas oryzae* pv. *oryzae* in rice. *Sci. Rep.* **6**, 26411. https://doi.org/10.1038/srep26411 (2016).
57. Ding, S. et al. Nitrogen forms and metabolism affect plant defence to foliar and root pathogens in tomato. *Plant. Cell. Environ.* **44**, 1596–1610. https://doi.org/10.1111/pce.14019 (2021).
58. Robatzek, S. & Somssich, I. E. Targets of AtWRKY6 regulation during plant senescence and pathogen defense. *Genes Dev.* **16**, 1139–1149. https://doi.org/10.1101/gad.222702 (2002).
59. Li, H. et al. WRKY transcription factors shared by BTH-induced resistance and NPR1-mediated acquired resistance improve broad-spectrum disease resistance in wheat. *MPMI* **33**, 433–443. https://doi.org/10.1094/mpmi-09-19-0257-r (2020).
60. Glazebrook, J. Contrasting mechanisms of defense against biotrophic and necrotrophic pathogens. *Annu. Rev. Phytopathol.* **43**, 205–227. https://doi.org/10.1146/annurev.phyto.43.040204.135923 (2005).
61. Brouwer, S. M. et al. Intact salicylic acid signalling is required for potato defence against the necrotrophic fungus *Alternaria solani*. *Plant. Mol. Biol.* **104**, 1–19. https://doi.org/10.1007/s11103-020-01019-6 (2020).
62. Kouzai, Y. et al. Salicylic acid-dependent immunity contributes to resistance against *Rhizoctonia solani*, a necrotrophic fungal agent of sheath blight, in rice and *Brachypodium distachyon*. *New. Phytol.* **217**, 771–783. https://doi.org/10.1111/nph.14849 (2018).
63. Ullah, C., Chen, Y. H., Ortega, M. A. & Tsai, C. J. The diversity of salicylic acid biosynthesis and defense signaling in plants: knowledge gaps and future opportunities. *Curr. Opin. Plant. Biol.* **72**, 102349. https://doi.org/10.1016/j.pbi.2023.102349 (2023).
64. Ullah, C., Schmidt, A., Reichelt, M., Tsai, C. J. & Gershenzon, J. Lack of antagonism between salicylic acid and jasmonate signalling pathways in Poplar. *New. Phytol.* **235**, 701–717. https://doi.org/10.1111/nph.18148 (2022).
65. Naidoo, R. et al. The identification and differential expression of *Eucalyptus grandis* pathogenesis-related genes in response to salicylic acid and methyl jasmonate. *Front. Plant. Sci.* **4**, 1–9. https://doi.org/10.3389/fpls.2013.00043 (2013).
66. Zwart, L. et al. Evidence for salicylic acid signalling and histological changes in the defence response of *Eucalyptus grandis* to *Chrysoporthe austroafricana*. *Sci. Rep.* **7**, 45402. https://doi.org/10.1038/srep45402 (2017).
67. Wilson, S. K., Pretorius, T. & Naidoo, S. Mechanisms of systemic resistance to pathogen infection in plants and their potential application in forestry. *BMC Plant. Biol.* **23**, 404. https://doi.org/10.1186/s12870-023-04391-9 (2023).
68. He, S. et al. Major latex protein MdMLP423 negatively regulates defense against fungal infections in Apple. *Int. J. Mol. Sci.* **21**, 1879. https://doi.org/10.3390/ijms21051879 (2020).
69. Choi, H. W. et al. A role for a menthone reductase in resistance against microbial pathogens in plants. *Plant. Physiol.* **148**, 383–401. https://doi.org/10.1104/pp.108.119461 (2008).
70. Marttinen, E. M. et al. Putative NAD (P)-binding Rossmann fold protein is involved in chitosan-induced peroxidase activity and lipoxygenase expression in *Physcomitrium patens*. *MPMI* **36**, 682–692. https://doi.org/10.1094/MPMI-07-23-0094-R (2023).
71. Huang, L. et al. NILR1 perceives a nematode ascaroside triggering immune signaling and resistance. *Curr. Biol.* **33**, 3992–3997. https://doi.org/10.1016/j.cub.2023.08.017 (2023).
72. Mendy, B. et al. *Arabidopsis* leucine-rich repeat receptor–like kinase NILR1 is required for induction of innate immunity to parasitic nematodes. *PLoS Pathog.* **13**, e1006284. https://doi.org/10.1371/journal.ppat.1006284 (2017).
73. Li, H. et al. A pathogenesis-related protein, PRP1, negatively regulates root nodule symbiosis in *Lotus japonicus*. *J. Exp. Bot.* **75**, 3542–3556. https://doi.org/10.1093/jxb/erae103 (2024).
74. Thumma, B. R., Sharma, N. & Southerton, S. G. Transcriptome sequencing of *Eucalyptus camaldulensis* seedlings subjected to water stress reveals functional single nucleotide polymorphisms and genes under selection. *BMC Genom.* **13**, 364. https://doi.org/10.1186/1471-2164-13-364 (2012).
75. Kriegshauser, L. et al. Function of the HYDROXYCINNAMOYL-CoA:SHIKIMATE HYDROXYCINNAMOYL TRANSFERASE is evolutionarily conserved in embryophytes. *Plant. Cell.* **33**, 1472–1491. https://doi.org/10.1093/plcell/koab044 (2021).
76. Dong, D. et al. Expression of a hydroxycinnamoyl-CoA shikimate/quinate hydroxycinnamoyl transferase 4 gene from *Zoysia Japonica* (*ZjHCT4*) causes excessive elongation and lignin composition changes in *Agrostis stolonifera*. *Int. J. Mol. Sci.* **23**, 9500. https://doi.org/10.3390/ijms23169500 (2022).
77. Karasov, T. L., Chae, E., Herman, J. J. & Bergelson, J. Mechanisms to mitigate the trade-off between growth and defense. *Plant. Cell.* **29**, 666–680. https://doi.org/10.1105/tpc.16.00931 (2017).
78. Djami-Tchatchou, A. T. et al. Dual role of auxin in regulating plant defense and bacterial virulence gene expression during *Pseudomonas syringae* PtoDC3000 pathogenesis. *MPMI* **33**, 1059–1071. https://doi.org/10.1094/MPMI-02-20-0047-R (2020).
79. Heidel, A. J., Clarke, J. D., Antonovics, J. & Dong, X. Fitness costs of mutations affecting the systemic acquired resistance pathway in *Arabidopsis thaliana*. *Genetics* **168**, 2197–2206. https://doi.org/10.1534/genetics.104.032193 (2004).
80. Van Hulten, M. et al. Costs and benefits of priming for defense in *Arabidopsis*. *PNAS* **103**, 5602–5607. https://doi.org/10.1073/pnas.0510213103 (2006).
81. Zas, R., Sampedro, L., Prada, E. & Fernandez-Lopez, J. Genetic variation of *Pinus pinaster* Ait. seedlings in susceptibility to the pine weevil *Hylobius abietis* L. *Ann. Sci.* **62**, 681–688. https://doi.org/10.1051/forest:2005064 (2005).
82. Di Matteo, G. & Voltas, J. Multienvironment evaluation of *Pinus pinaster* provenances: evidence of genetic trade-offs between adaptation to optimal conditions and resistance to the maritime pine Bast scale (*Matsucoccus feytaudi*). *Sci.* **62**, 553–563. https://doi.org/10.5849/forsci.15-109 (2016).
83. Climent, J. et al. Trade-offs and trait integration in tree phenotypes: consequences for the sustainable use of genetic resources. *Curr. Rep.* **10**, 196–222. https://doi.org/10.1007/s40725-024-00217-5 (2024).

Acknowledgements
The authors would like to thank Dr Raphael Ployet, Dr Kathleen Marchal, Dr Erik Visser and Prof. Tuan Duong for their assistance with the data analysis, bioinformatic support and manuscript input.

Author contributions
S.S. designed the analysis framework, performed data analyses, prepared all figures and wrote the initial draft. S.N. conceived the study, secured funding and contributed to manuscript revision. All authors read and approved the final manuscript.

Funding
This work was supported by the South African National Research Foundation (NRF) doctoral support to SS (PMDS240903265966). The authors acknowledge funding from the Technology Innovation Agency (TIA) and the Department of Science, Technology and Innovation (DSTI) through the Forest Bioeconomy Innovation Cluster Programme 1 to SN and SS. Opinion expressed and conclusions arrived at, are those of the authors and are not necessarily to be attributed to the NRF.

Declarations

Competing interests
The authors declare no competing interests.

Additional information
Supplementary Information The online version contains supplementary material available at https://doi.org/10.1038/s41598-025-32699-z.

Correspondence and requests for materials should be addressed to S.N.

Reprints and permissions information is available at www.nature.com/reprints.

Publisher's note Springer Nature remains neutral with regard to jurisdictional claims in published maps and institutional affiliations.